Supplementary Note

Physics-Informed Neural Operators for Generalizable and Label-Free Inference of Temperature-Dependent Thermoelectric Properties

Hyeonbin Moon[1†], Songho Lee[1†], Wabi Demeke[1†,*], Byungki Ryu[2], Seunghwa Ryu[1*]

Affiliations

[1]Department of Mechanical Engineering, Korea Advanced Institute of Science and Technology (KAIST), 291 Daehak-ro, Yuseong-gu, Daejeon 34141, Republic of Korea

[2]Energy Conversion Research Center, Korea Electrotechnology Research Institute (KERI), 12 Jeongiui-gil, Seongsan-gu, Changwon-si, Gyeongsangnam-do 51543, Republic of Korea

[†]These authors contributed equally to this work

[*]Corresponding authors: wabi@kaist.ac.kr and ryush@kaist.ac.kr

Keywords: Thermoelectric properties (TEPs), PDEs, forward/inverse problem, PINNs, PINOs

Supplementary Note 1. Comparison of 1D versus 2D

While a one-dimensional (1D) assumption was adopted to evaluate the field variables of thermoelectric (TE) materials, we validated the validity of this simplification by comparing it against two-dimensional (2D) simulations. Specifically, the 1D PINN model solution was copied in the y-direction and compared with full 2D finite element analysis (FEA) results. As shown in **Fig. S1(a–c)** for temperature and **Fig. S1(d–f)** for voltage, the predictions from the 1D PINN model closely match the corresponding 2D FEA solutions. This agreement supports the validity of the 1D approximation to higher dimensions. Notably, the critical aspect of solving TE systems lies in accurately capturing the temperature and voltage gradients along the direction of heat and current flow, especially for temperature-dependent TE material properties.

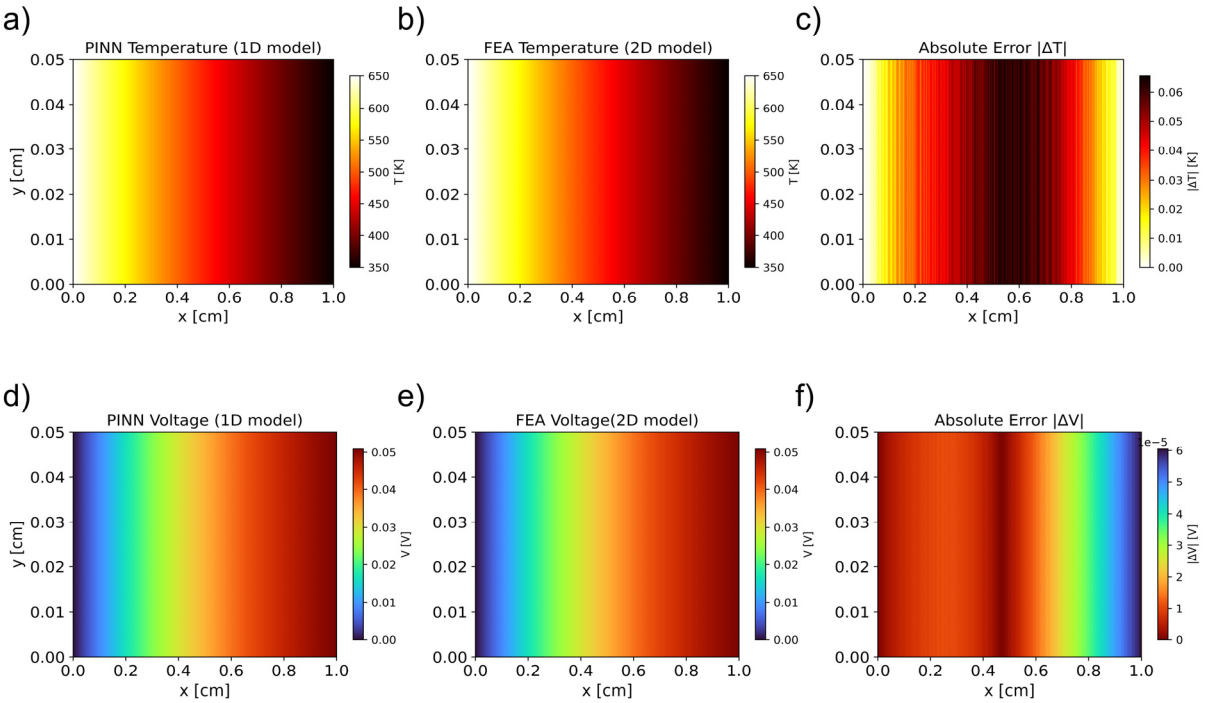

Fig. S1 (a) Temperature fields obtained by 1-PINN model by simply copying in y-direction. (b) the temperature fields obtained by 2-D analysis of FEA. (c) temperature difference between PINN vs 2-D FEA models. (d) voltage fields obtained by 1-PINN model by simply copying in y-direction. (b) the voltage fields obtained by 2-D analysis of FEA. (c) voltage difference between PINN vs 2-D FEA models.

Supplementary Note 2. Ill-posedness of inverse problem

We consider the steady-state thermoelectricity in one dimension, governed by the following coupled differential equations:

$$\frac{\mathrm{d}}{\mathrm{dx}}\left(-\sigma(T)\frac{dV}{dx}+\alpha(T)\frac{dT}{dx}\right)=0 \tag{1a}$$

$$\frac{\mathrm{d}}{\mathrm{dx}}\left(\alpha(T)T\left(-\sigma(T)\frac{dV}{dx}+\alpha(T)\frac{dT}{dx}\right)-k(T)\frac{dT}{dx}\right)=-\frac{dV}{dx}\left(-\sigma(T)\frac{dV}{dx}+\alpha(T)\frac{dT}{dx}\right) \tag{1b}$$

subject to the boundary conditions:

$$T(x=0)=T_h, \qquad T(x=L)=T_h \tag{1c}$$

$$V(x=0)=0, \qquad J(x=L)=J_{applied} \tag{1d}$$

Suppose the spatial profiles $T(x)$ and $V(x)$ are fully known from measurements. The inverse problem then aims to identify the three temperature-dependent material properties $\sigma(T)$, $k(T)$ and $\alpha(T)$. However, the direct identification is fundamentally ill-posed, as the system provides only two scalar equations at each spatial point while requiring the estimation of three unknown functions.

To address this underdetermination, two assumptions are introduced. First, the temperature-dependent electrical conductivity $\sigma(T)$ is assumed to be fully known from independent measurements, thereby reducing the number of unknowns from three to two. Second, to supplement the boundary information, it is assumed that the thermal conductivity $k(T)$ is known at a specific reference temperature T_0.

Under these assumptions, the inverse problem reduces to determining two unknown functions, $k(T)$ and $\alpha(T)$, based on the two governing differential equations (Eqs. (1a) and (1b)) and two boundary-related constraints: the prescribed current density $J(x=L)=J_{applied}$

and the known value $k(T_0)$. This formulation ensures that the number of independent constraints matches the number of unknowns, thereby leading to a mathematically well-posed inverse problem. The assumptions of known $\sigma(T)$ and $k(T_0)$ arise directly from the mathematical structure of the governing system and are essential for preventing non-uniqueness and ensuring the identifiability of the material properties.

Supplementary Note 3. PINN/PINO architecture and input encoding

As shown in **Fig. S2,** all networks are 6-layer multilayer perceptron's (MLPs) with 32 nodes per layer and hyperbolic tangent (Tanh) activation. The forward PINN uses a single network. The inverse PINN uses two networks with identical structure. The inverse PINO consists of four networks—two branches and two trunks—with shared architecture but different inputs. All models were trained using the Adam optimizer with a fixed learning rate of 1×10^{-4}

For the inverse PINO, each branch network receives an 11-dimensional input vector explicitly defined as

$$\{T^1_{measure}, T^2_{measure}, T^3_{measure}, V^1_{measure}, V^2_{measure}, V^3_{measure}, \sigma_1, \sigma_2, \sigma_3, \sigma_4, k(T_0)\}$$

Here, $T^i_{measure}, V^i_{measure} (i = 1,2,3)$ represent sparse point measurements of temperature and voltage along the spatial domain. The coefficients σ_1 to σ_4 correspond to a third-order polynomial approximation of the temperature-dependent electrical conductivity $\sigma(T)$, providing a simplified representation of its variation with temperature. The final term $k(T_0)$ provides a known single value of thermal conductivity. All input features are non-dimensionalized to ensure numerical stability and consistent scaling during training.

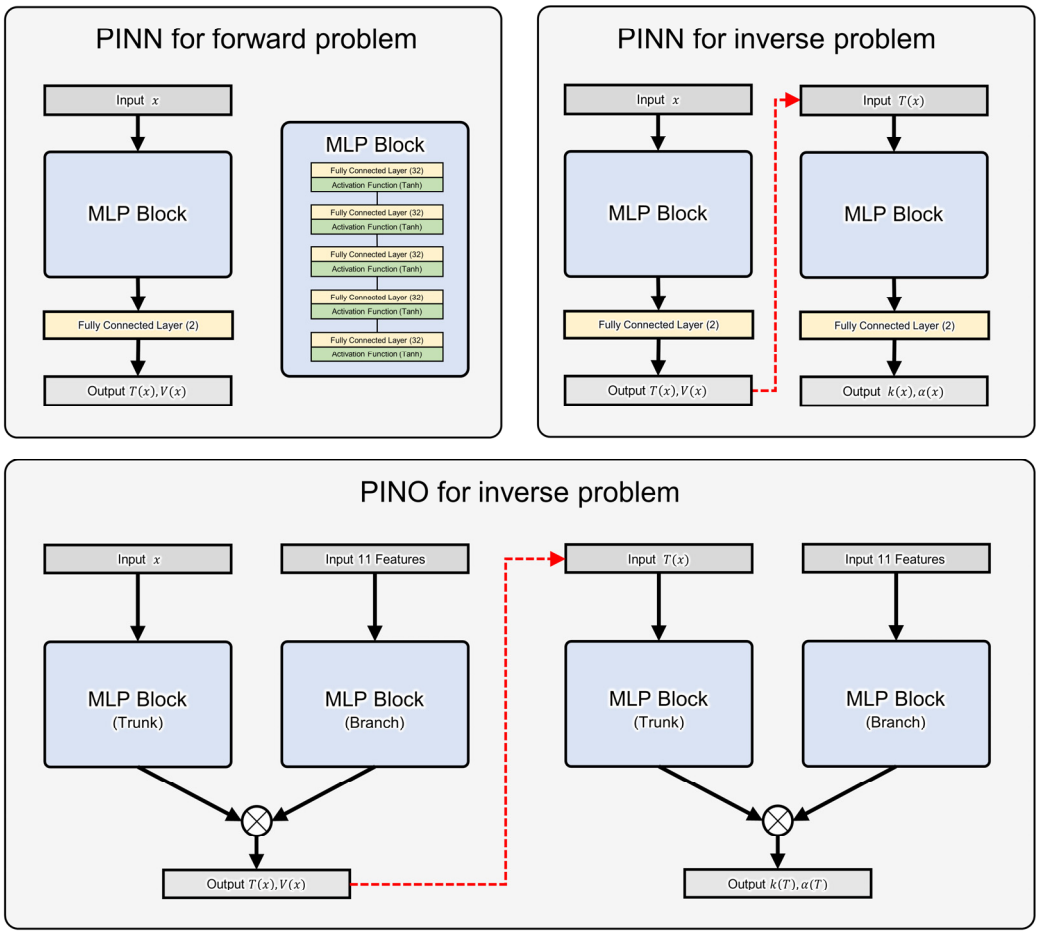

Fig. S2 Architectures of PINN and PINO used for forward and inverse problems.

Supplementary Note 4. Data augmentation for PINO training

The input features to the branch networks in the PINO framework consist of eleven elements: three sparse temperature measurements $T(x)$, three sparse voltage measurements $V(x)$, four coefficients of a third-order polynomial fit to the electrical conductivity $\sigma(T)$, and a known value of thermal conductivity $k(T_0)$ at $T_0 = 350K$. Thus, each training sample can be represented as a vector in $\boldsymbol{R}^{11}$. To enable supervised-free learning across multiple material systems, twenty distinct material cases were initially selected from the available dataset, providing a set of base inputs $\{\mathbf{y_i}\}_{i=1}^{20}$, where each $\mathbf{y_i} \in \boldsymbol{R}^{11}$. These base cases were generated based solely on physical measurements $\left(\mathrm{T}, \mathrm{V}, \sigma(\mathrm{T}), \mathrm{k}(\mathrm{T_0})\right)$ without reference to ground truth thermal conductivity $k(T)$ or Seebeck coefficient $\alpha(\mathrm{T})$ during training.

However, training PINO solely on these 20 samples resulted in insufficient generalization capability. To overcome this, data augmentation was introduced by applying random perturbations to the input features. Specifically, each input feature $\mathrm{y_{ij}}$ was independently multiplied by a random scaling factor $r_{ij} \sim Uinform(0.7,1.3)$, leading to augmented inputs of the form:

$$\widehat{y_{ij}} = r_{ij} \times y_{ij} \quad for\ i = 1, \dots, 20\ \ and\ \ j = 1, \dots, 11$$

This augmentation process was repeated 49 times, producing approximately 1000 perturbed samples in total for training.

It is important to note that augmentation was performed by perturbing the physically realizable base cases rather than randomly sampling arbitrary feature vectors. Direct random sampling of temperature and voltage measurements, along with $\sigma(T)$and $k(T_0)$ values, could result in non-physical or inconsistent data that does not correspond to any realizable set of thermoelectric material properties. Such inconsistencies would introduce noise into the training

process and deteriorate model performance. By perturbing existing physically meaningful samples, we ensured that all augmented inputs remained within a physically feasible regime, allowing PINO to learn inverse mappings robustly.

Supplementary Note 5. Comparison with purely data-driven approach

Typical data-driven approaches rely on labeled datasets during training. While standard PINO does not have access to full $\kappa(T)$ and $\alpha(T)$ curves, it can reconstruct complete temperature-dependent profiles using only sparse field measurements and known electrical conductivity. To highlight the limitations of purely data-driven methods, we trained a multi-layer perceptron (MLP) using sparse measurements from 20 TE materials, including $\sigma(T)$ and a single thermal conductivity value, as inputs to predict the full $\kappa(T)$ and $\alpha(T)$ curves (**Fig. S3(a)**). The model was then tested on 60 unseen materials. As shown in **Fig. S3(b)** and **S3(c)**, the MLP overfits the training data and fails to generalize, demonstrating the limitations of data-driven models when labeled data are limited.

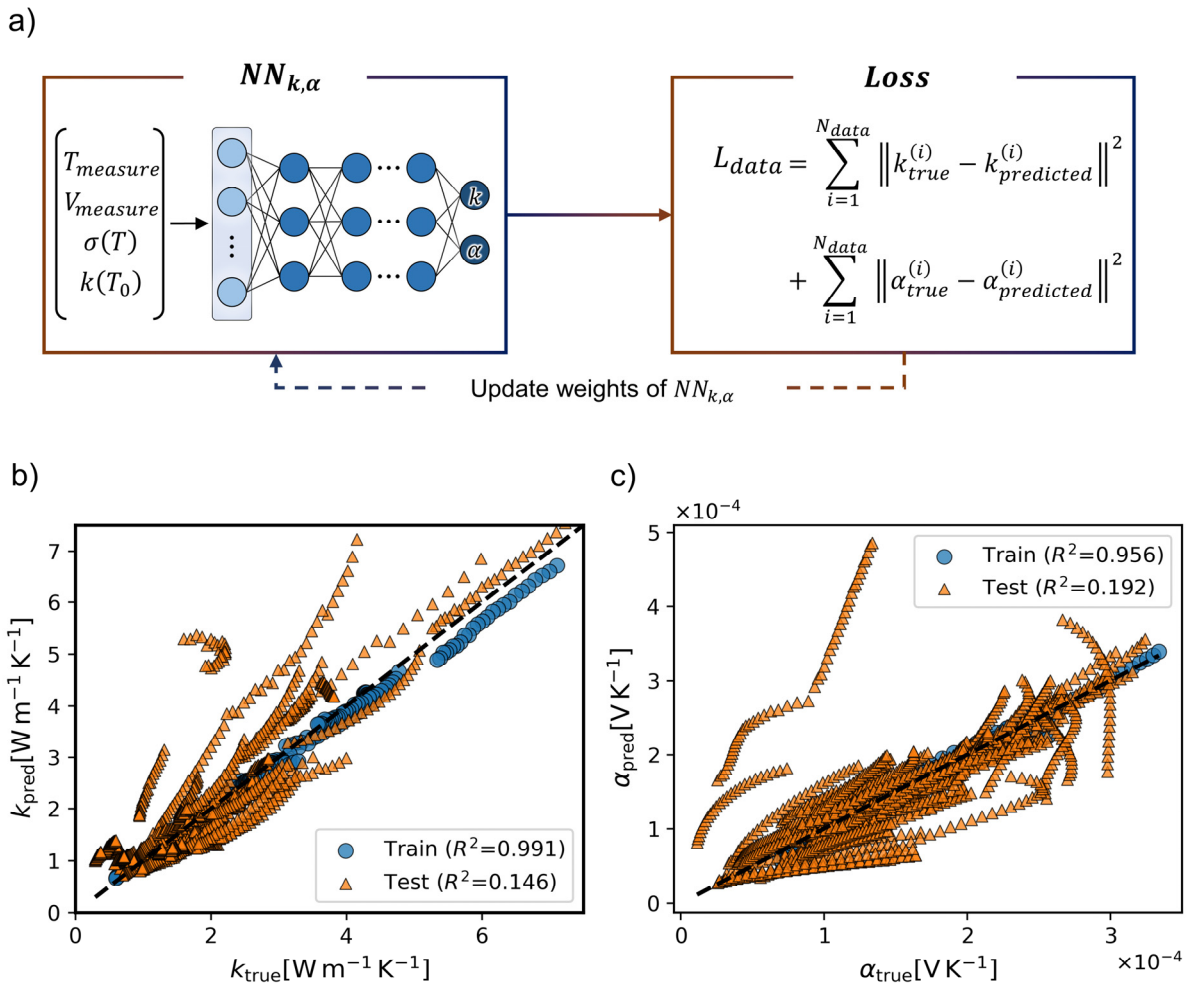

Fig. S3 (a) Training of the MLP model fully data-driven approach (b) and (c) Comparison between predicted and true values for the training and test sets, for thermal conductivity and Seebeck coefficient, respectively.